

# Effect of Nanostructures Addition and Enhancement of Poly (Vinylidene Difluoride) (PVDF) Energy Harvesting

Omar Peña-Oliveras<sup>1</sup>, Brenda Javier-Boodhan<sup>1</sup>, Anthony La Santa<sup>1</sup>, Juan Gonzalez-Sanchez<sup>2</sup>

<sup>1</sup>Division of Science, Technology and Engineering, Universidad Ana G. Méndez, Carolina Campus, Carolina, Puerto Rico

<sup>2</sup>Department of Electronics, University of Puerto Rico, Bayamon Campus, Bayamon, Puerto Rico

Email: [juan.gonzalez19@upr.edu](mailto:juan.gonzalez19@upr.edu)

**How to cite this paper:** Peña-Oliveras, O., Javier-Boodhan, B., La Santa, A. and Gonzalez-Sanchez, J. (2024) Effect of Nanostructures Addition and Enhancement of Poly (Vinylidene Difluoride) (PVDF) Energy Harvesting. *Materials Sciences and Applications*, 15, 228-244.  
<https://doi.org/10.4236/msa.2024.157016>

**Received:** June 5, 2024

**Accepted:** July 20, 2024

**Published:** July 23, 2024

Copyright © 2024 by author(s) and Scientific Research Publishing Inc. This work is licensed under the Creative Commons Attribution International License (CC BY 4.0).

<http://creativecommons.org/licenses/by/4.0/>



Open Access

## Abstract

With concerns in energy crisis and global warming, researchers are actively investigating alternative energy renewable solutions. Among the various methods, piezoelectric transduction stands out due to its impressive electromechanical coupling factor and coefficient. As a result, piezoelectric energy harvesting has garnered significant attention from the scientific community. In this study, we explored methods to enhance the piezoelectric properties of polyvinylidene fluoride (PVDF) through two distinct approaches. The first approach involved applying external high voltages at various stages during the mixture reaction. The goal was to determine whether this voltage application could alter or enhance PVDF's piezoelectric conformation by improving the alignment of polarized dipoles. In the second part of our study, we investigated the effects of incorporating various nanostructures (including Iron Oxide, Magnesium Oxide, and Zinc Oxide) into PVDF. To analyze changes in PVDF's crystalline structure, we utilized Fourier Transform Infrared Spectroscopy (FTIR) and X-ray Diffraction (XRD) techniques. Additionally, we measured the electric polarization of samples using a Precision LC Meter and examined the morphology of nanofibers through Scanning Electron Microscopy (SEM).

## Keywords

Poly (Vinylidene Fluoride) (PVDF), Energy Harvesting, Electrospinning, Nanoparticles, ZnO, MgO, Fe<sub>3</sub>O<sub>4</sub>

## 1. Introduction

Traditional energy sources, such as fossil fuels, are finite and harm the environ-

ment. Energy harvesting offers a solution by harnessing abundant, renewable resources. By reducing our dependence on non-renewable fuels, we actively combat climate change and promote sustainability. Energy scavenging, also known as ambient power or harvesting, involves capturing small amounts of ambient energy (such as light, heat, or vibration) and converting it into electricity. This technology has promising applications in remote or inaccessible areas where traditional energy sources are impractical. This innovation drives progress across various fields, from smart cities to healthcare, for instance, it could power biosensors within the human body [1]. The ability to harness energy from the environment opens new possibilities for sustainable and self-sufficient devices. The amount of energy and performance of these harvesting devices depends strongly on specific properties of materials such as piezoelectricity [2].

Polyvinylidene fluoride (PVDF) is a high-purity and non-reactive thermoplastic fluoropolymer, that has great chemical resistance, piezoelectric properties, high mechanical strength and good processability. PVDF has four main crystalline phases known as  $\alpha$ ,  $\beta$ ,  $\gamma$ ,  $\delta$  [3]. The most stable and frequent is the  $\alpha$ -phase, which crystallizes in an orthorhombic cell, where two chains are packed oppositely, canceling the individual dipole moments. Many of the properties of PVDF, those associated with its use as a sensor or actuator, are linked to the electrical dipole moment of the PVDF monomer unit about  $(5-8 \times 10^{-30} \text{ cm})$  which is due to the electronegativity of fluorine atoms as compared to those of hydrogen and carbon atoms [4]. The  $\beta$  and  $\gamma$  are considered the most electrically active phases directly related to piezoelectricity of the polymer, but the  $\beta$ -phase has the highest spontaneous polarization in all these four phases, because of the dipole arrangement. The  $\gamma$  conformation is also considered an electrically active phase, but not as much as the  $\beta$  phase. By analyzing the  $\gamma$  phase, two opposite chains conform to a monoclinic crystal lattice, where only a fraction of dipole moments are cancelled. The  $\gamma$  phase can be obtained by melting or crystallizing the polymer at temperatures near the melt temperature of the  $\alpha$ -phase or over  $165^\circ\text{C}$  [5]. The  $\delta$  phase is formed when the  $\alpha$  phase is electrically poled, and one of the chains aligns parallel to the other, resulting in a weak net dipole moment. The crystal lattice parameters are identical to the  $\alpha$  phase [6]. One of our research goals is to create a material capable of powering body biosensors or IoT, enhancing the beta phase conformation of PVDF is crucial. By optimizing this phase, we cover the way for efficient energy conversion and sustainable applications.

One of the research ideas for energy harvesting involves adding nanoparticles to PVDF, aiming to boost the energy production of the polymer or enhance its piezoelectricity or expand it toward ferroelectricity. The incorporation of ZnO nanoparticles into PVDF can significantly impact the content of the  $\beta$  phase [7]. This influence arises from the promotion of crystallization, alignment of polymer chains, and nucleation of the  $\beta$  phase. These effects play a crucial role in

customizing PVDF-ZnO composites to achieve specific piezoelectric properties tailored for various applications. Researchers frequently investigate and optimize the ZnO loading to strike the right balance between enhanced piezoelectric performance and practical material processing considerations. These nanoparticles (NPs) have outstanding results in increasing the ability to harvest mechanical energy from body movement [8]. When this component is incorporated with other polymers such as PVDF into the electrospinning technique, the crystalline beta phase improves resulting in the piezoelectric properties of the “nanofiber mats” [8]. Increasing the amount of ZnO nanoparticles is directly proportional to the enhancement in the beta phase of PVDF [2]. Magnesium oxide (MgO) is another chemical that has outstanding properties to harvest mechanical energy. This chemical is odorless, non-toxic and has a high hardness, purity, and melting point. The MgO in PVDF matrix has a low frequency in electronic applications [9]. When MgO is in a PVDF matrix, it shows a dielectric increment in the  $\beta$  phase. Iron oxide ( $\text{Fe}_3\text{O}_4$ ) nanoparticles have improved ferroelectric properties that make this happen [10].

## 2. Materials

The PVDF utilized in our study was Sigma – Aldrich (182702) white powder. The solvents also manufactured by Sigma-Aldrich Acetone and DMF used was Chromasol® 99.9%. The syringes for the polymeric solutions are a 1/2 cc Becton Dickinson with needle length of 13 mm and a diameter of 0.40 mm. For the Electrospinning procedure, a metal support was used to maintain the syringes. A heating mantle was placed under the syringe to maintain the desired temperature for the polymeric solutions. The power supply for electrospinning is a BT-GP-AC-30P30 Benchtop Universal AC input, 30 KV, 30 W. The Scanning Electron Microscope, JEOL JSM-6010LA. The X-Ray Diffraction is Rigaku Xtal-Lab Supernova single crystal X-ray Diffraction system and Radiant RT66C Ferroelectric Test System. For capacitor synthesis, we used an in-house designed customized multilayer contact with a thickness of 1 mm with different areas. The MgO nanoparticles are from Nanostructured & Amorphous Materials, 99% pure with an average particle size 20 nm and ellipsoidal & spherical shapes. The ZnO and  $\text{Fe}_3\text{O}_4$  nanoparticles are from US Research Nanomaterials, 99% pure with average particle size of 35 - 45 nm and 98% pure and 20-30 nm respectively.

## 3. Experimental

Morell and his group conducted a study on the evolution of polycrystalline diamond using ellipsometry [11]. By analyzing the evolution of the obtained patterns, they could determine the optimal stage for synthesizing the diamond. Although we currently lack an ellipsometer, this led us to consider applying high voltages at different stages of our solution’s reaction. We posed the following research question: Can we enhance the piezoelectric response by applying high voltages at different stages of the reaction? If such an improvement occurs,

which of these voltages would be optimal for promoting the beta phase? This inquiry served as a preamble to the initial part of our study.

**Process 1:** The solutions were prepared by diluting polyvinylidene fluoride (PVDF) diluted in Acetone with different weight percent (wt%) (7, 10, 15 and 20). Two sets of samples were prepared samples, one with applied high voltage since the beginning of the mixing process and other sets, without the high voltage to the solution as shown in **Figure 1**. These samples were collocated on a hot plate and stirred for 4 hours. After the mixing process is completed, we measure every solution on the FTIR Spectrometer and apply a force of 100N, get the background and obtain the data of the transmittance from 400 to 1000  $\text{cm}^{-1}$ . The  $\alpha$ -phase has bands at 614, 764 and 976  $\text{cm}^{-1}$  of the spectra [12] [13]. Characteristic bands of  $\beta$  - phase, responsible for the piezoelectric properties on PVDF are in the 445, 510 and 840  $\text{cm}^{-1}$  [14]. The  $\gamma$  - phase can be found at 431, 512, 776, 812 and 833  $\text{cm}^{-1}$  peaks [15] [16]. Later, we prepared the polymeric solution for the electrospinning process. We observed a solidification of the solution at room temperature and to solve the issue, we added a heating mantle below the syringe to maintain the temperature of the solution over 35°C. We proceeded to connect the high voltage power supply, the positive onto the syringe needle negative onto the metallic collector. We used voltage variations from 500VDC up to 15,000VDC. The obtained nanofibers were characterized with Scanning Electron Microscope (SEM), we observed the nanofibers shapes, sizes, diameters, and investigated their homogeneity.

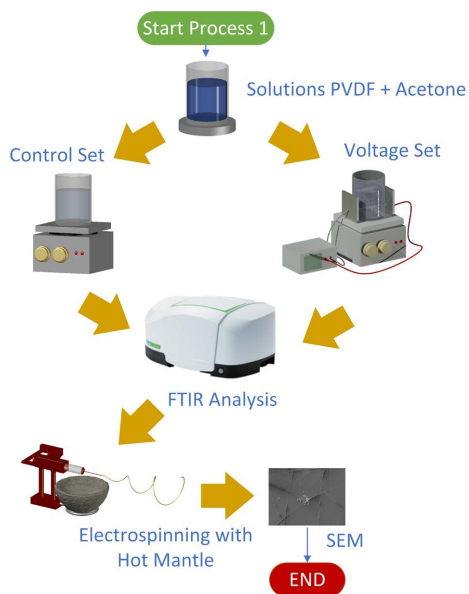


**Figure 1.** Methodology set up for PVDF + acetone polymeric solutions.

Gonzalez and his group observed that iron oxide and PVDF nanofibers introduced magnetic hysteresis but did not significantly enhance the piezoelectric properties of PVDF [17]. Consequently, we aimed to verify whether certain vari-

ation to these nanoparticles could indeed improve piezoelectricity. Furthermore, we aimed to validate existing literature that emphasizes ZnO's positive impact on enhancing PVDF's piezoelectric behavior. We also explored the incorporation of MgO nanoparticles into PVDF for enhancing dielectric performance, breakdown strength, and energy storage capabilities.

**Process 2:** Initially, acetone was replaced with Dimethylformamide (DMF), a more effective solvent, to dissolve PVDF in solutions at different weight percentages (wt%), specifically 8%, 10%, 15%, and 20%, to serve as the control group. Separate batches were prepared by adding different types of nanoparticles—ZnO, Fe<sub>3</sub>O<sub>4</sub>, and MgO—to the PVDF solution as shown in **Figure 2**. The ratio of nanoparticles to PVDF varied across five different proportions: 1:1, 1:5, 1:10, 1:15, and 1:20. These mixtures were then placed on a hot plate with a stirring mechanism and heated for 2 hours at a constant speed of 300 revolutions per minute (rpm). This step ensures uniform distribution of nanoparticles and aids in the formation of a homogeneous solution. The samples were subjected to various characterization techniques. FTIR was used to identify the chemical structures, X-Ray Diffraction (XRD) to determine the crystalline structure, and Liquid Crystal (LC) Analyzer to assess the electrical properties. After characterization, the solutions were prepared for electrospinning and then to the SEM to analyze their surface morphology and structure.

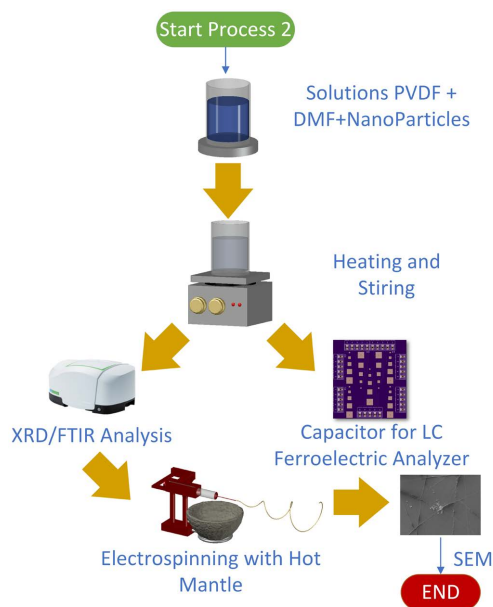


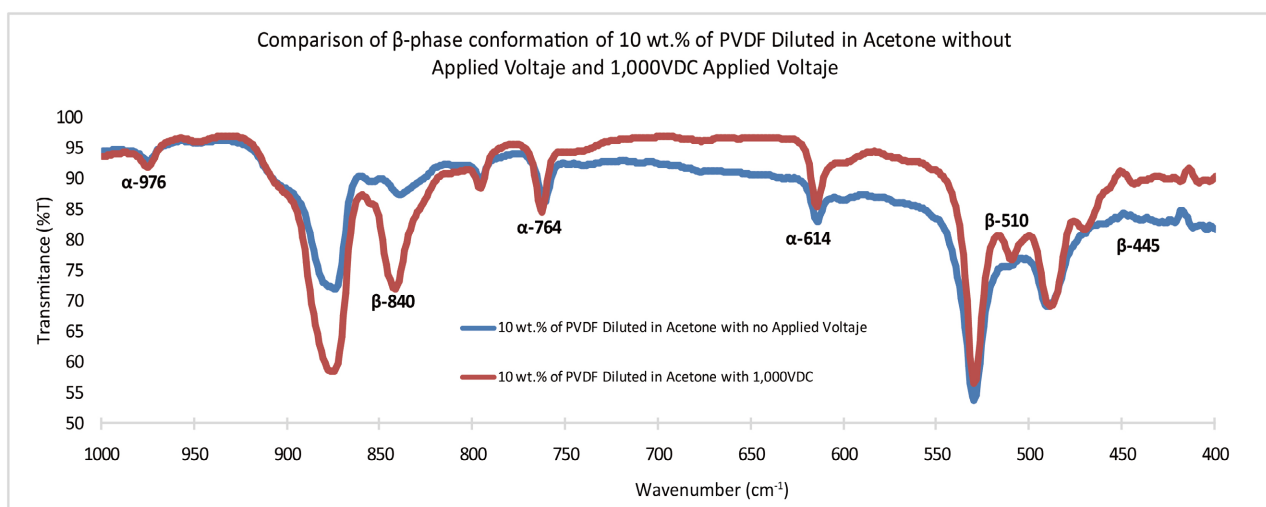
**Figure 2.** Methodology set up for PVDF + DMF polymeric solutions with ZnO, MgO and Fe<sub>3</sub>O<sub>4</sub>.

## 4. Results and Analysis

### 4.1. Process 1: FTIRs of Solutions with PVDF and Acetone with High Voltage

We will present the 10% weight solutions, but similar results were observed with

the others wt%. In this parameter, we observed better nanoparticles distribution. **Figure 3(a)** compares results of PVDF diluted with acetone at 10 wt% with 1000 V and the ones with no voltage resulting in a change conformation in the  $\beta$ -phase peaks of 510 and 840  $\text{cm}^{-1}$ . The bands related to the  $\beta$ -phase are deeper than the ones with the  $\alpha$ -phase. **Figure 3(b)** shows similar behavior, but also an increase in the 445  $\text{cm}^{-1}$   $\beta$ -phase peak no present in the 1,000 volts samples. Possible reasons for this change in crystalline conformation may be attributed to polarization effects. The application of the electric field improves the alignment of the polymer chains, thereby positively influencing the beta conformation. Also, the formation of the  $\beta$ -phase is related mainly to the evaporation rate of the solvents [14]. Low evaporation rates result predominantly in the  $\beta$ -phase, thermodynamically more favorable, intermediate rates in a mixture of  $\alpha$  and  $\beta$  and high rates in the  $\alpha$ -phase, kinetically more favorable [15]. In literature and by experience, acetone is not an appropriate solvent to promote the formation of the  $\beta$ -phase, but with the high voltage, the acetone can do enhance the PVDF piezoelectricity no matter the evaporation rate. The combined effect of solvent and electric field might induce a phase transition in PVDF, leading to changes in the characteristic peaks. As we increase the voltage over 15 kilovolts this effect of changing the conformations to the beta phase is lost despite having more energy to move the loads (**Figure 3(c)**). As voltage increases, several factors come into play. Dielectric breakdown disrupts the ordered arrangement of polymer chains, affecting the  $\beta$ -phase conformation. Additionally, electrode polarization becomes dominant, hindering the desired alignment. Excessive voltage can lead to material degradation, altering crystalline phases (Xu, 2014). Surface charge accumulation near electrodes may also impact PVDF behavior. It is possible that the dipolar moment decreases with the voltage intensity. The best parameters for optimization of the  $\beta$ -phase conformation of PVDF are between 1000 to 5000 volts right at the beginning of mixing the PVDF with the acetone.



(a)

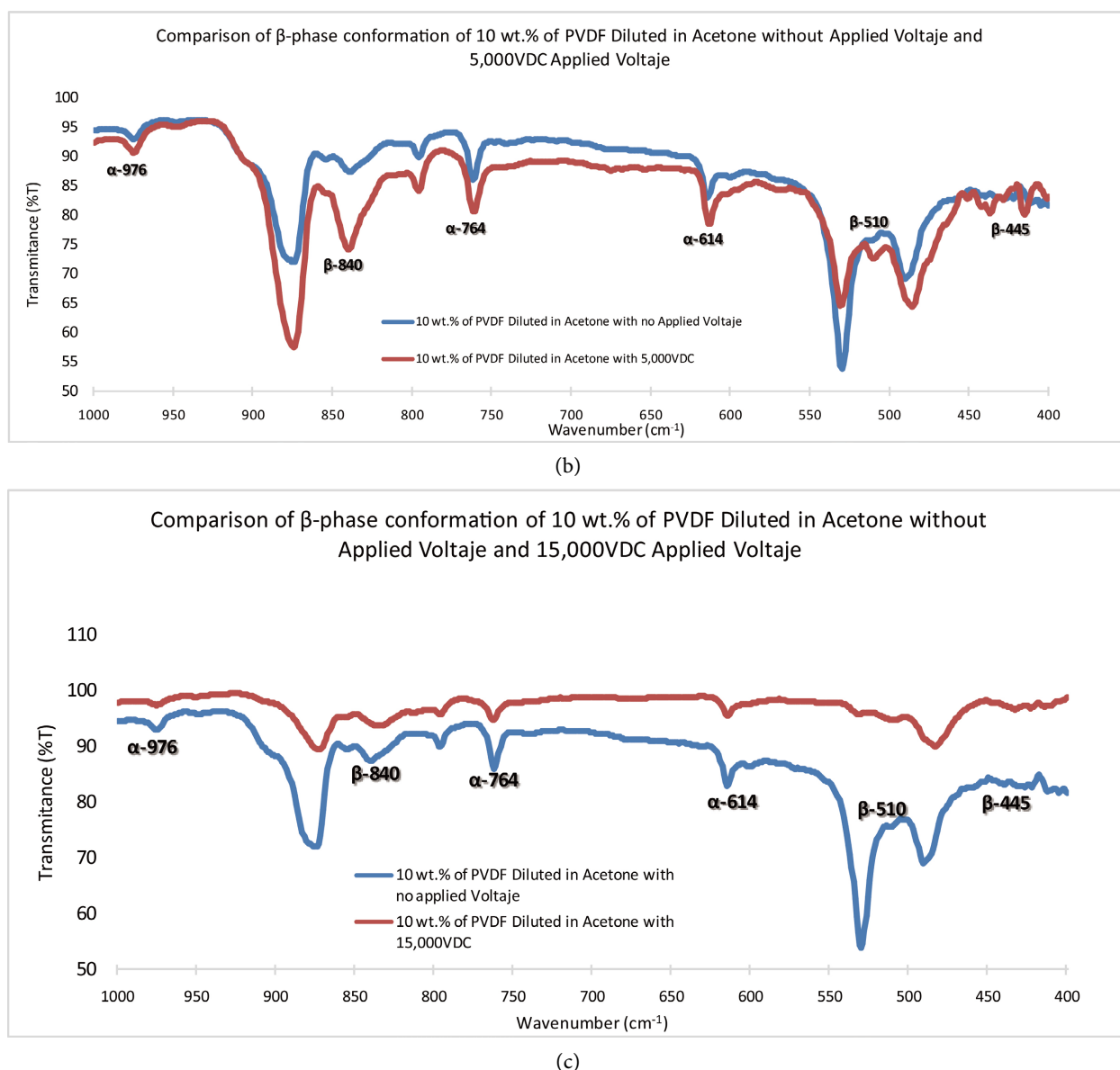


**Figure 3.** Comparison of  $\beta$ -phase conformation of 10 wt% of PVDF diluted in acetone without applied voltage and voltage of 1000 V, 5000 V and 15,000 V.

#### 4.2. Process 2: FTIRs of Solutions Containing Nanoparticles

In **Figure 4**, we show FTIR spectra of the general or average behavior that we obtained from PVDF solutions containing one of the proposed nanoparticles (ZnO, MgO and Fe<sub>3</sub>O<sub>4</sub>). The results presented correspond to the 15 wt% case, where nanofibers exhibit improved uniformity and homogeneity. At the top of the graph is the zinc oxide solution with a ratio of 1:15, then in the center is iron oxide with a ratio of 1:5 and finally magnesium oxide (1:10) at the bottom. These samples were our best  $\beta$ -peaks for these nanoparticles with no voltage. The samples do not reveal a great change in the conformation of the beta phase, but if we look closely at the 840  $\text{cm}^{-1}$  peak, ZnO nanoparticles slightly affect the conformation as mentioned by other scientists in the literature.

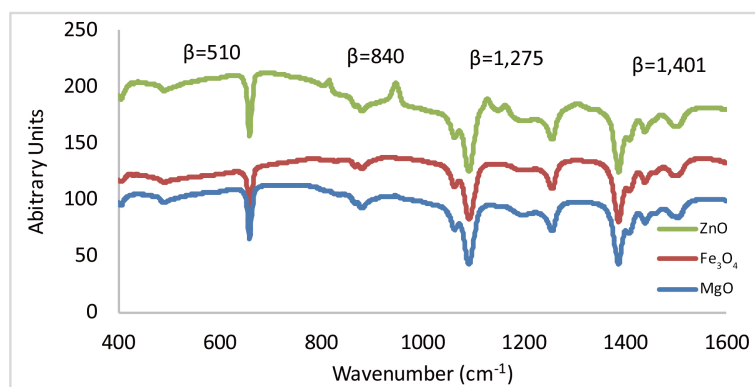


**Figure 4.** FTIR spectra of solutions PVDF with ZnO (Top), Fe<sub>3</sub>O<sub>4</sub> (Center) and MgO (Bottom).

### 4.3. X-Ray Diffraction (XRD)

XRD analysis has been useful to determine the PVDF crystalline phases [18], [19]. Even with the  $\alpha$  (17.66°, 18.30°, 19.9° and 26.56°),  $\beta$  (20.26°) and  $\gamma$  (18.5°, 19.2° and 20.04°) phases presenting similar peaks, some of them are exclusive for each phase allowing better characterization. We first observed the X-ray diffraction of the compounds in their pure form, taking first the PVDF and then all the nanoparticles in the study. **Figure 5** shows the alpha conformation wrapping the PVDF with a bandwidth from 18.30° to 26.56°, also presence of the  $\beta$ -phase at 20.26° and gamma at 20.04°. Thus, it is possible to conclude that the PVDF used in our experiments has some dipole moment for the intrinsic piezoelectricity, but most of the conformation is mostly associated to alfa phase. **Figure 6** shows the Fe<sub>3</sub>O<sub>4</sub> nanoparticles analysis, the peaks indexed as planes (220) at 31.5°, (311) at 36.4°, (400) at 43.5°. These planes are distinctive of a cubic spinel structure [20], which is expected. The narrow peaks on spectra points to the formation of some nanocluster structures of Fe<sub>3</sub>O<sub>4</sub> nanoparticles. **Figure 7** shows peaks for MgO nanoparticles at 18.57°, 36.96°, 38.02°, and 42.98°, corresponding to planes (111), (002), (202), (113), [21] the MgO nanoparticles are polycrystalline. **Figure 8** shows the ZnO diffraction pattern, and the peaks located at 31.84°,

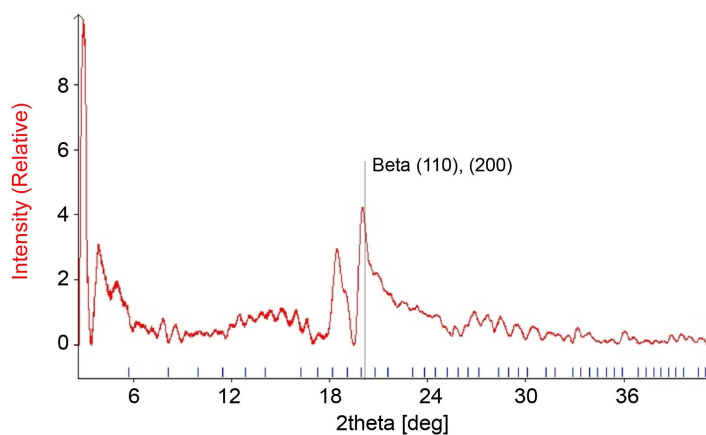


**Figure 5.** XRD of the sigma – Aldrich (182702) PVDF powder.

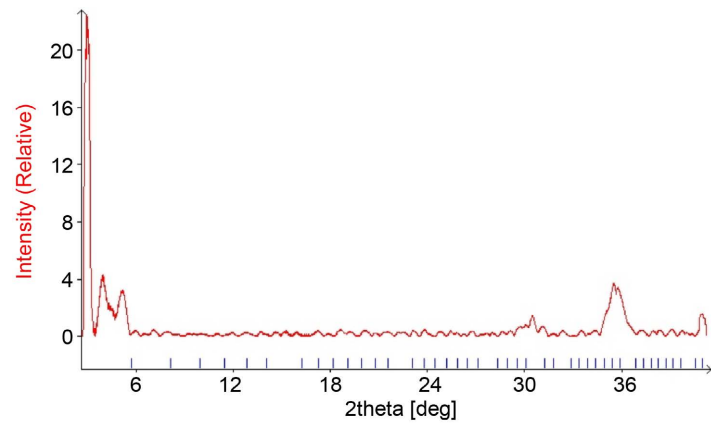


**Figure 6.** Fe<sub>3</sub>O<sub>4</sub> nanoparticles from US research nanomaterials.

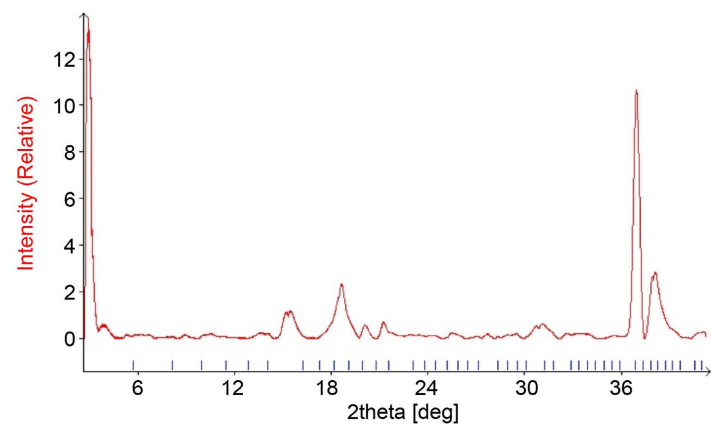


**Figure 7.** MgO nanoparticles from US research nanomaterials.

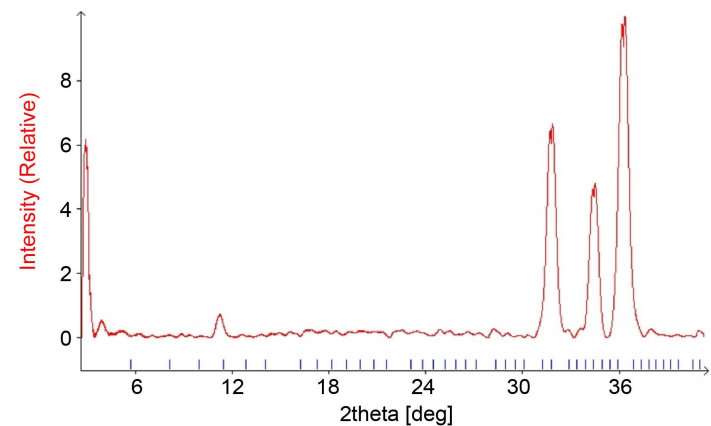


**Figure 8.** ZnO nanoparticles from US research nanomaterials.

34.52°, 36.33° which corresponds to planes (100), (002) and (101) [22]. It is worth noting that the XRD peaks for the nanoparticles are located far from those of the PVDF, which makes it easier to detect any change in conformation.

The next step was to analyze thin films of our solutions after they had dried resulting with a texture very similar to that of Teflon. The XRDs are from the samples that were made at 15 wt%, because they have resulted in much better

solutions for electrospinning and the quality of the fibers. **Figure 9** shows  $\text{Fe}_3\text{O}_4$  and PVDF in 1:5 proportion, if we compare it with the spectrum of pure PVDF in **Figure 5**, we can observe that the width of the beta and gamma peaks are much more pronounced, which is indicative that there was a change in the conformation of the sample towards to a better piezoelectricity.

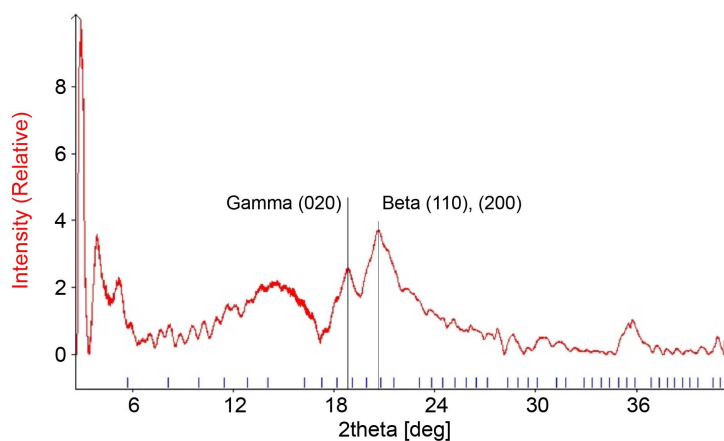


**Figure 9.** XRD  $\text{Fe}_3\text{O}_4$  with PVDF in a proportion 1:5.

**Figure 10** shows  $\text{MgO} + \text{PVDF}$  at a 1:10 ratio, this time the peak is much more intense near  $20.26^\circ$  than the XRD of pure PVDF (**Figure 5(a)**) and consistent with what was observed from the FTIR in **Figure 4**.

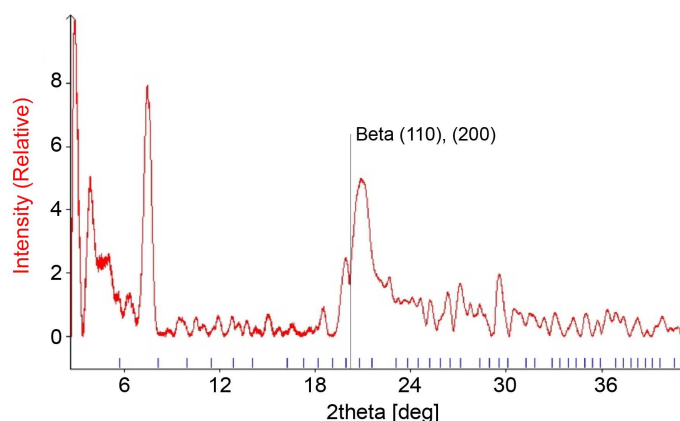


**Figure 10.** XRD  $\text{MgO}$  with PVDF in proportion 1:10.

Scientists have reported improvement in the piezoelectric properties of PVDF by adding nanoparticles of  $\text{ZnO}$  [8], but in the spectrum of  $\text{ZnO} + \text{PVDF}$  at a 1:15 ratio, it can be observed (**Figure 11**) that there is not much variation in the beta peaks than the spectrum of pure PVDF.

#### 4.4. Precision LC Ferroelectric Tester

To measure ferroelectricity, we created capacitors by placing the solutions to dry inside small molds one millimeter thick in contacts created in our laboratory on

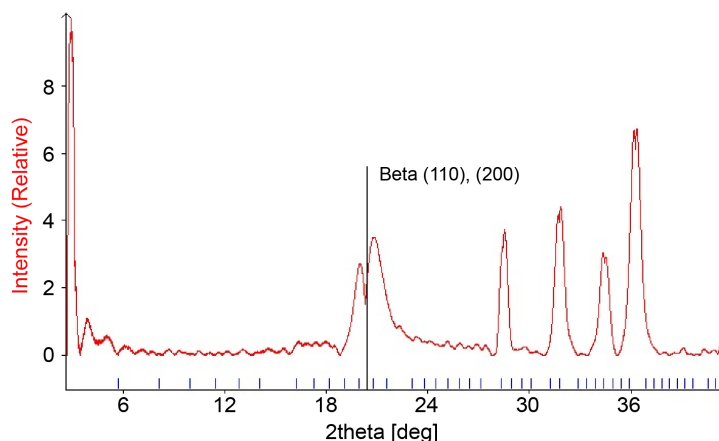
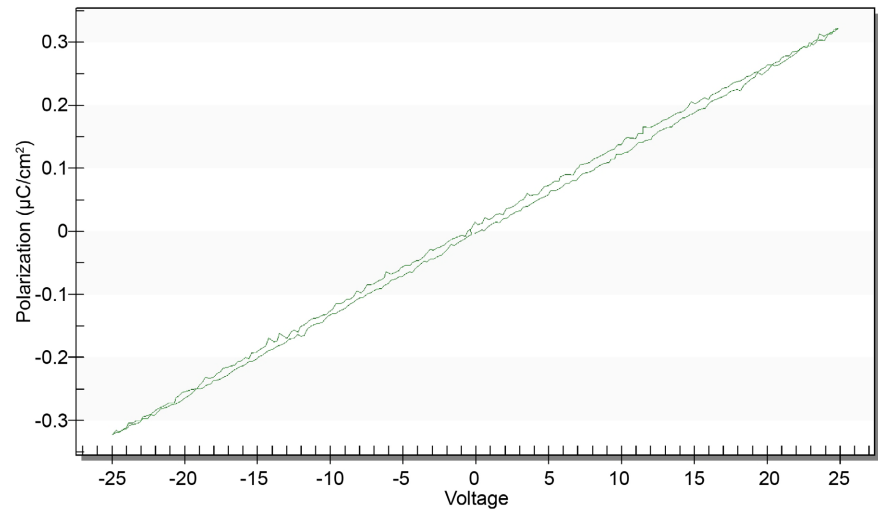


**Figure 11.** XRD ZnO with PVDF in proportion 1:15.

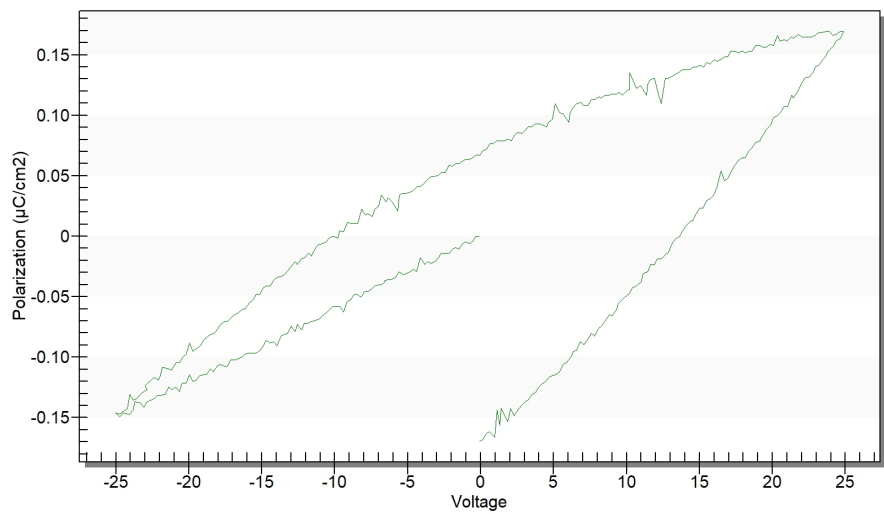
a printed circuit board. As expected, the pure PVDF of **Figure 12(a)** has dielectric polarization. PVDF has a dielectric constant of 7.8 which makes it a good material for capacitors. Magnetite ( $\text{Fe}_3\text{O}_4$ ) is an intriguing material with both magnetic and electrical properties, but it is not inherently multiferroic. The addition of  $\text{Fe}_3\text{O}_4$  nanoparticles to PVDF caused almost linear hysteresis with polarization values degenerating near zero voltage (**Figure 12(b)**). A change in the properties of PVDF is evident just when it is in the presence of the  $\text{Fe}_3\text{O}_4$  nanoparticles changing the linear pattern that dielectrics exhibit. Although a full ferroelectric pattern is not observed, the change in the dielectric constant due to the addition of  $\text{Fe}_3\text{O}_4$  suggests that this material's behavior could be attributed to several factors, such as the introduction of defects, strain, or changes in the electronic structure that affect the polarization response of the material [23]. It is also possible that  $\text{Fe}_3\text{O}_4$  nanoparticles could interact with the host PVDF lattice in a manner that mimics towards a ferroelectric behavior. Gonzalez *et al.* demonstrated that PVDF containing  $\text{Fe}_3\text{O}_4$  nanoparticles exhibited ferromagnetic hysteresis properties [17].

**Figure 13(a)** presents results with the addition of MgO nanoparticles to PVDF improving the dielectric constant. Tiantian, *et al.* has shown that incorporating MgO nanofillers into PVDF can significantly improve its dielectric constant and breakdown strength [24]. This is attributed to the nanoparticles' ability to suppress space charge accumulation, which in turn reduces dielectric loss and increases the material's electrical stability. The addition of MgO nanoparticles enhances PVDF's dielectric efficiency, improving energy storage and release. This enhancement is particularly beneficial for applications in energy storage devices, where high dielectric performance is crucial.

ZnO has a long history as an electronic material, because of its large piezoelectric constant useful for ultrasonic transducers, solar cells, transparent conductors, and gas sensors [25] [26]. In the literature, no evidence has been found that ZnO has ferroelectric properties, if it has been found with variations doped with lithium [27]. **Figure 13(b)** illustrates an unexpected polarization pattern in the

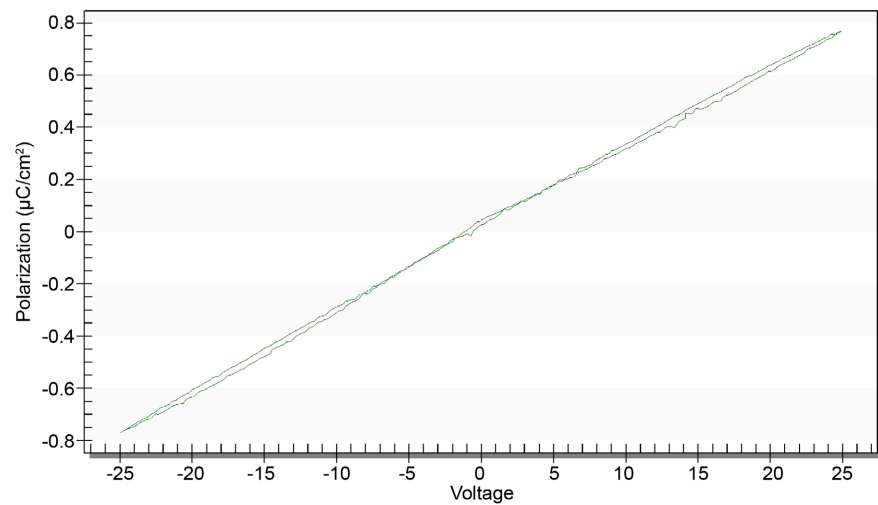


(a)



(b)

**Figure 12.** LC Ferroelectric results (a) PVDF sample dissolve on DMF, (b) PVDF +  $\text{Fe}_3\text{O}_4$  Nanoparticles in a proportion 1:5.



(a)

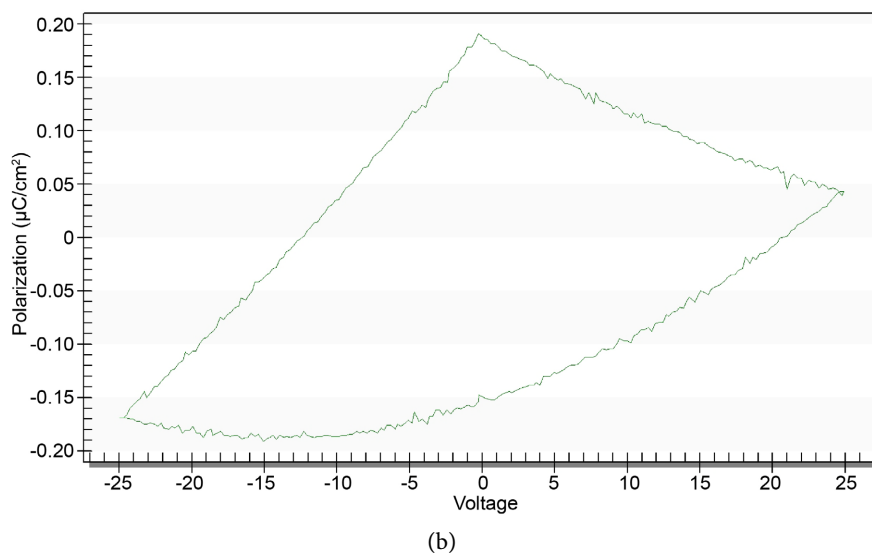


**Figure 13.** LC ferroelectric results, (a) MgO with PVDF in proportion 1:10, (b) ZnO with PVDF in proportion 1:15.

composite of ZnO and PVDF. Despite multiple repetitions of the experiment, this anomalous behavior persisted, indicating this consistent triangle like polarization. The consistent occurrence of this phenomenon suggests that it may be an inherent characteristic of the ZnO-PVDF composite, potentially arising from unique interactions between the ZnO nanoparticles and the PVDF matrix. After reviewing the literature, we did not find any similar behavior, leading us to conclude that this variation results in an unusual yet convenient type of polarization. This result may hold significance for electronic applications, as it exhibits an inversely proportional variation with a positive voltage, coupled with second-order behavior, and conversely, the opposite occurs with negative voltage.

#### 4.5. Scanning Electron Microscope (SEM)

To perform the SEMs, we analyzed the powders in their 99% pure form and **Figure 10** provides insights into the composition of our core materials. **Figure 14(a)** illustrates the typical appearance of PVDF, while **Figure 14(b)** reveals the presence of microparticles in iron oxide. Interestingly, the MgO (14C) and ZnO (14D) samples exhibit nanoscale features. During electrospinning, solutions of 7 and 8 wt% of PVDF diluted in acetone and DMF respectively resulted in splattered droplets, which were due to the solution being too liquid, and less viscous. We noted that the wt% was not ideal for the formation of homogenous fibers, the electrospinning process should be initiated at a higher wt%. Solutions at 10 wt% with both solvents were tested, the collection process was easier and less droplets were produced and presented more of a structure than the 7 and 8 wt%.

The solutions of 15 wt% on acetone or DMF would present better results than the first two mentioned earlier, the nanofibers collected improved homogeneity and no droplets, indicating that this concentration is the optimum for synthesis.

In **Figure 15(a)**, we can see the result of a 15% solution of PVDF diluted in acetone from process 1 with nanofibers from 250 nm to 1000 nm. With the PVDF and the iron nanoparticles (**Figure 15(b)**), a polymeric mesh with many fibers was formed. It is good to mention that the PVDF with iron oxide moves when being impacted by the electron beam of the SEM, another data that supports the improvement of the piezoelectricity of PVDF. Samples with MgO and PVDF

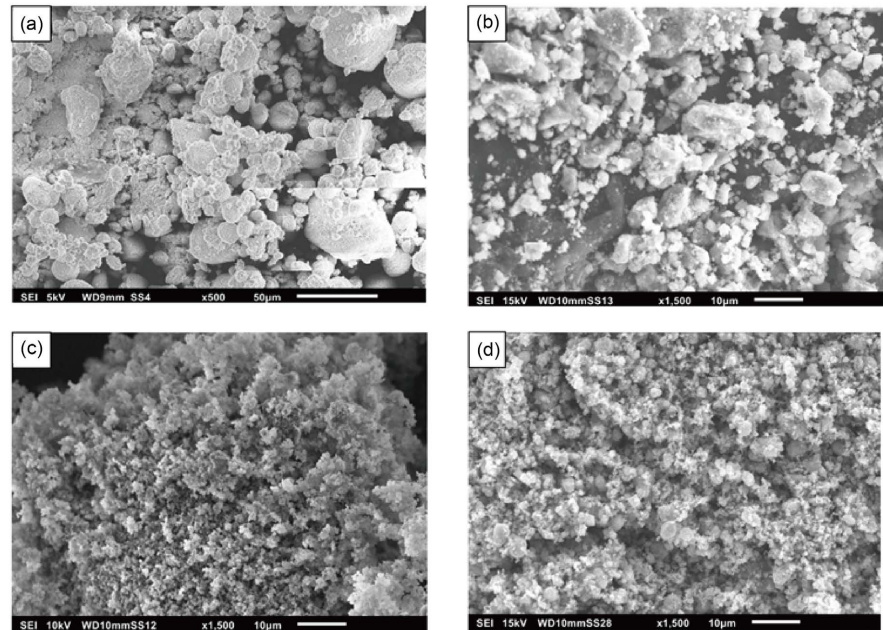


**Figure 14.** Morphology of PVDF powder (a), Fe<sub>3</sub>O<sub>4</sub> NPs (b), MgO NPs (c), ZnO NPs (d).

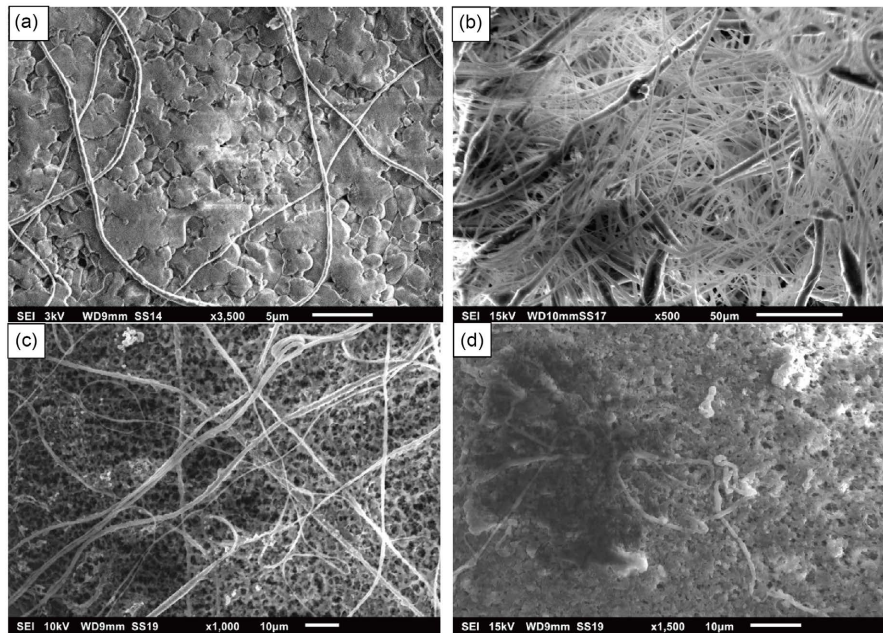


**Figure 15.** Morphology of the electrospinning of our solutions, (a) 15 wt% of PVDF in Acetone (Process 1), (b) 15 wt% Fe<sub>3</sub>O<sub>4</sub> NPs + PDVF 1:5 ratio, (c) 15 wt% MgONPs + PVDF 1:10 ratio and (d) 15 wt% ZnO NPs + PVDF 1:15 ratio.

(**Figure 15(c)**) made it possible to obtain fibers from 500 nm to 1,200 nm. No movement of these fibers was observed when the electron beam hit them. In the case of the solutions with ZnO and PVDF (**Figure 15(d)**) it was difficult to achieve many fibers with electrospinning. It is possible that the DMF will not dissolve the ZnO completely and make the process a little more difficult to achieve. What we were able to observe was the movement of the fibers when we felt the SEM beam.

## 5. Conclusion

It is possible to Enhance  $\beta$ -phase Conformation by using High Voltage during the entire solution reaction time and create better piezoelectric and energy harvesting nanofibers. FTIRs of samples showed an enhancement on voltages from 1000 to 5000 volts. Voltages over 10,000 V risk damaging the material as the dielectric threshold disrupts PVDF's polymer chain order and  $\beta$ -phase structure. Electrode polarization then becomes predominant, opposing chain alignment and  $\beta$ -phase development. This resulting finding is excellent for scalability because it does not involve high costs to enhance the piezoelectric and energy harvesting performance. Traditional polarization and synthetic copolymers are typically used, but they can be costly due to high polymerization expenses and the limited crystallinity of copolymers. The crystalline conformation of the PVDF is a clear combination of the  $\alpha$ ,  $\beta$  and  $\gamma$  phases according to FTIR and XRD results. The polarization of the thin films in the capacitors revealed dielectric behavior in PVDF, with an observed enhancement in the dielectric constant upon the addition of MgO nanoparticles. The incorporation of Fe<sub>3</sub>O<sub>4</sub> nanoparticles into PVDF leads to an almost linear hysteresis in polarization, particularly as values approach zero voltage. This indicates that Fe<sub>3</sub>O<sub>4</sub> nanoparticles alter PVDF's typical dielectric pattern. While not fully ferroelectric, the modified dielectric constant implies that Fe<sub>3</sub>O<sub>4</sub>'s presence affects PVDF's polarization, potentially due to introduced defects, strain, or electronic structure changes. The addition of ZnO nanoparticles to PVDF displayed a unique, triangular polarization pattern that remained consistent across multiple experiments. This suggests an inherent property of the composite, likely due to specific interactions between ZnO nanoparticles and the PVDF matrix. Literature review revealed no similar behavior, indicating that this distinctive polarization could be advantageous for electronic applications, especially as it shows an inversely proportional response to positive voltage and second-order behavior, with the reverse effect under negative voltage.

## Acknowledgements

To Namir Huertas and Dr. Lisandro Cunci from UAGM Campus for the assistance in the logistic and SEM images. A huge thank you to the US Department of Education for funding the MSEIP R3 STEM Research (P120A160126) and the Project HSI-STEM (P031C160222). Special thanks to Jean Gonzalez for his help with Powder X-Ray Diffraction and Dr. Dalice Piñero for her support with the

facilities at UPR Molecular Science Research Center.

## Conflicts of Interest

The authors declare no conflicts of interest regarding the publication of this paper.

## References

- [1] Xue, Z., Wu, L., Yuan, J., Xu, G. and Wu, Y. (2023) Self-Powered Biosensors for Monitoring Human Physiological Changes. *Biosensors*, **13**, Article 236. <https://doi.org/10.3390/bios13020236>
- [2] Golmohammadi Rostami, S., Sorayani Bafqi, M.S., Bagherzadeh, R., Latifi, M. and Gorji, M. (2015) Multi-layer Electrospun Nanofiber Mats with Chemical Agent Sensor Function. *Journal of Industrial Textiles*, **45**, 467-480. <https://doi.org/10.1177/1528083715601507>
- [3] Lovinger, A.J. (1983) Ferroelectric Polymers. *Science*, **220**, 1115-1121. <https://doi.org/10.1126/science.220.4602.1115>
- [4] Giannetti, E. (2001) Semi-crystalline Fluorinated Polymers. *Polymer International*, **50**, 10-26. [https://doi.org/10.1002/1097-0126\(200101\)50:1<10::aid-pi614>3.0.co;2-w](https://doi.org/10.1002/1097-0126(200101)50:1<10::aid-pi614>3.0.co;2-w)
- [5] Gregorio Jr., R. and Cestari, M. (1994) Effect of Crystallization Temperature on the Crystalline Phase Content and Morphology of Poly (Vinylidene Fluoride). *Journal of Polymer Science Part B: Polymer Physics*, **32**, 859-870. <https://doi.org/10.1002/polb.1994.090320509>
- [6] Schwartz, M. (2002) Encyclopedia of Smart Materials. Wiley. <https://doi.org/10.1002/0471216275>
- [7] Singh, H.H., Singh, S. and Khare, N. (2017) Enhanced  $\beta$ -Phase in PVDF Polymer Nanocomposite and Its Application for Nanogenerator. *Polymers for Advanced Technologies*, **29**, 143-150. <https://doi.org/10.1002/pat.4096>
- [8] Jin, C., Hao, N., Xu, Z., Trase, I., Nie, Y., Dong, L., *et al.* (2020) Flexible Piezoelectric Nanogenerators Using Metal-Doped ZnO-PVDF Films. *Sensors and Actuators A: Physical*, **305**, Article ID: 111912. <https://doi.org/10.1016/j.sna.2020.111912>
- [9] Rozana, M.D., Arshad, A.N., Wahid, M.H., Habibah, Z., Ismail, L.N., Sarip, M.N., *et al.* (2012). Dielectric Constant of PVDF/MgO Nanocomposites Thin Films. 2012 *IEEE Symposium on Business, Engineering and Industrial Applications*, Bandung, 23-26 September 2012, 18-22. <https://doi.org/10.1109/isbeia.2012.6422866>
- [10] Gao, X., Liang, S., Ferri, A., Huang, W., Rouxel, D., Devaux, X., *et al.* (2020) Enhancement of Ferroelectric Performance in PVDF: Fe<sub>3</sub>O<sub>4</sub> Nanocomposite Based Organic Multiferroic Tunnel Junctions. *Applied Physics Letters*, **116**, Article ID: 152905. <https://doi.org/10.1063/1.5145316>
- [11] Morell, G., Cancel, L.M., Figueroa, O.L., González, J.A. and Weiner, B.R. (2000) Structural Evolution during Chemical Vapor Deposition of Diamond Thin Films. *Journal of Applied Physics*, **88**, 5716-5719. <https://doi.org/10.1063/1.1313783>
- [12] Gregorio, R. (2006) Determination of the  $\alpha$ ,  $\beta$ , and  $\gamma$  Crystalline Phases of Poly (Vinylidene Fluoride) Films Prepared at Different Conditions. *Journal of Applied Polymer Science*, **100**, 3272-3279. <https://doi.org/10.1002/app.23137>
- [13] Kobayashi, M., Tashiro, K. and Tadokoro, H. (1975) Molecular Vibrations of Three Crystal Forms of Poly (Vinylidene Fluoride). *Macromolecules*, **8**, 158-171. <https://doi.org/10.1021/ma60044a013>

- [14] Gregorio, R. and Borges, D.S. (2008) Effect of Crystallization Rate on the Formation of the Polymorphs of Solution Cast Poly (Vinylidene Fluoride). *Polymer*, **49**, 4009-4016. <https://doi.org/10.1016/j.polymer.2008.07.010>
- [15] Costa, L.M.M., Bretas, R.E.S. and Gregorio, R. (2010) Effect of Solution Concentration on the Electrospray/Electrospinning Transition and on the Crystalline Phase of PVDF. *Materials Sciences and Applications*, **1**, 247-252. <https://doi.org/10.4236/msa.2010.14036>
- [16] Xu, F., Chen, X. and Wang, N. (2024) PVDF Crystalline Phases Revisited: A First-Principles Computational Study Using the PBE-D3 Functional. *Journal of Polymer Research*, **31**, Article No. 112. <https://doi.org/10.1007/s10965-024-03968-8>
- [17] Gonzalez, J.A., Furlan, R., Lopez, R., Martinez, L.M. and Fachini, E. (2014) Magnetic Field Assisted Electrospinning of Nanofibers Using Solutions with PVDF and Fe<sub>3</sub>O<sub>4</sub> Nanoparticles. *MRS Proceedings*, **1659**, 155-162. <https://doi.org/10.1557/opl.2014.210>
- [18] Martins, P., Costa, C.M. and Lanceros-Mendez, S. (2010) Nucleation of Electroactive  $\beta$ -Phase Poly (Vinylidene Fluoride) with CoFe<sub>2</sub>O<sub>4</sub> and NiFe<sub>2</sub>O<sub>4</sub> Nanofillers: A New Method for the Preparation of Multiferroic Nanocomposites. *Applied Physics A*, **103**, 233-237. <https://doi.org/10.1007/s00339-010-6003-7>
- [19] Martins, P., Lopes, A.C. and Lanceros-Mendez, S. (2014) Electroactive Phases of Poly (Vinylidene Fluoride): Determination, Processing and Applications. *Progress in Polymer Science*, **39**, 683-706. <https://doi.org/10.1016/j.progpolymsci.2013.07.006>
- [20] Kim, Y.I., Kim, D. and Lee, C.S. (2003) Synthesis and Characterization of CoFe<sub>2</sub>O<sub>4</sub> Magnetic Nanoparticles Prepared by Temperature-Controlled Coprecipitation Method. *Physica B: Condensed Matter*, **337**, 42-51. [https://doi.org/10.1016/s0921-4526\(03\)00322-3](https://doi.org/10.1016/s0921-4526(03)00322-3)
- [21] Balakrishnan, G., Velavan, R., Mujasam Batoo, K. and Raslan, E.H. (2020) Microstructure, Optical and Photocatalytic Properties of MgO Nanoparticles. *Results in Physics*, **16**, Article ID: 103013. <https://doi.org/10.1016/j.rinp.2020.103013>
- [22] Zhou, J., Zhao, F., Wang, Y., Zhang, Y. and Yang, L. (2007) Size-Controlled Synthesis of ZnO Nanoparticles and Their Photoluminescence Properties. *Journal of Luminescence*, **122**, 195-197. <https://doi.org/10.1016/j.jlumin.2006.01.089>
- [23] Singh, S. and Goswami, N. (2021) Structural, Optical, Magnetic and Dielectric Properties of Magnetite (Fe<sub>3</sub>O<sub>4</sub>) Nanoparticles Prepared by Exploding Wire Technique. *Journal of Materials Science: Materials in Electronics*, **32**, 26857-26870. <https://doi.org/10.1007/s10854-021-07062-3>
- [24] Yan, T.T., Wen, Y., Liu, J., Liao, H. and Zhang, J. (2022) A Brief Overview of the Optimization of Dielectric Properties of PVDF and Its Copolymer-Based Nanocomposites as Energy Storage Materials. *Polymer Science, Series A*, **64**, 393-405. <https://doi.org/10.1134/s0965545x22700146>
- [25] Klingshirn, C.F., Meyer, B.K., Waag, A., Hoffmann, A. and Geurts, J. (2010) Zinc Oxide from Fundamental Properties towards Novel Applications. Springer. <https://doi.org/10.1007/978-3-642-10577-7>
- [26] Tsukazaki, A., Ohtomo, A., Onuma, T., Ohtani, M., Makino, T., Sumiya, M., *et al.* (2004) Repeated Temperature Modulation Epitaxy for P-Type Doping and Light-Emitting Diode Based on ZnO. *Nature Materials*, **4**, 42-46. <https://doi.org/10.1038/nmat1284>
- [27] Zhang, S.B., Wei, S.H. and Zunger, A. (2001) Intrinsic N-Type versus P-Type Doping Asymmetry and the Defect Physics of ZnO. *Physical Review B*, **63**, Article ID: 075205. <https://doi.org/10.1103/physrevb.63.075205>